# Mass estimates for very cold (

J. Steinacker, H. Linz, H. Beuther, Th. Henning, A. Bacmann

A&A 593, L5 (2016)
DOI: 10.1051/0004-6361/201629068


Astronomy & Astrophysics

Letter to the Editor

# Mass estimates for very cold (<8 K) gas in molecular cloud cores

J. Steinacker[1,2,3], H. Linz[3], H. Beuther[3], Th. Henning[3], and A. Bacmann[1,2]

[1] Univ. Grenoble Alpes, IPAG, 38000 Grenoble, France
[2] CNRS, IPAG, 38000 Grenoble, France
[3] Max-Planck-Institut für Astronomie, Königstuhl 17, 69117 Heidelberg, Germany
e-mail: stein@mpia.de

Received 7 June 2016 / Accepted 9 August 2016

**ABSTRACT**

*Context.* The mass of prestellar cores is an essential ingredient to understand the onset of star formation in the core. The low level of emission from cold dust may keep parts of this dust hidden from observation.
*Aims.* We aim to determine the fraction of core mass in the temperature range <8 K that can be expected for typical low- and high-mass star formation regions.
*Methods.* We calculated the dust temperature within standard spherically symmetric prestellar cores for a grid of density power laws in the outer core regions, core masses, and variations in the external multicomponent radiation field. We assume the dust is composed of amorphous silicate and carbon and we discuss variations of its optical properties. As a measure for the distribution of cores and clumps, we used core mass functions derived for various environments. In view of the high densities in very cold central regions, dust and gas temperatures are assumed to be equal.
*Results.* We find that the fraction of mass with temperatures <8 K in typical low- and high-mass cores is <20%. It is possible to obtain higher fractions of very cold gas by placing intermediate- or high-mass cores in a typical low-mass star formation environment. We show that the mass uncertainty arising from far-infrared to mm modeling of very cold dust emission is smaller than the mass uncertainty owing to the unknown dust opacities.
*Conclusions.* Under typical star formation conditions, dust with temperatures <8 K covers a small mass fraction in molecular cloud cores, but may play a more important role for special cases. The major unknown in determining the total core mass from thermal dust emission is the uncertainty in the dust opacity, not in the underestimated very cold dust mass.

**Key words.** radiative transfer – radiation mechanisms: thermal – stars: formation – ISM: clouds

## 1. Introduction

While molecular cloud cores have been identified as the site where the star formation starts, which physical processes initiate and control the onset is still a matter of debate. To assess the impact of effects such as gravitational instability or shielding from the outer radiation field, the spatial mass distribution of the core is one of the key ingredients to progress to a paradigm. Since molecules tend to freeze out onto the dust grains in the shielded cold core center with temperature around 10 K, thermal emission from dust is the main tool to determine the core structure and its mass.

Accumulated for an entire star formation region, the numbers of cores in a certain mass range can aid the understanding of the overall efficiency of the star formation process when compared to the initial mass function of stars (e.g., Motte et al. 1998; Alves et al. 2007). Könyves et al. (2010), for example, have determined such a core mass function (CMF) for Aquila based on single-temperature modified blackbody fits of the dust emission maps. Also, CMFs were derived for cores in a massive star formation environment (e.g., for Orion A North; Nutter & Ward-Thompson 2007). Computationally, more costly improvements to the single-temperature approach consider a spherical or elliptical core model with a radial dust temperature profile (Evans et al. 2001; Zucconi et al. 2001; Shirley et al. 2005; Nielbock et al. 2012; Launhardt et al. 2013; Roy et al. 2014; Steinacker et al. 2016). Already in the early work by Evans et al. (2001) and Zucconi et al. (2001), the dust temperature distribution of prestellar cores is calculated self-consistently by illuminating the core with an external radiation field. Zucconi et al. (2001) proposed a multicomponent model of the interstellar radiation field (ISRF) based on the data given in Black (1994). In their discussion they stressed that the model likely underestimates both the far-infrared (FIR) and mid-infrared (MIR) field caused by local sources such as thermal emission from big dust grains or small stochastically-heated grains (SHG). Without this component, Zucconi et al. derived temperatures <8 K for core regions with visual extinction >30 mag. They concluded that the emission seen in FIR maps may be dominated by the contribution from the low-density exterior of the core.

The argument was repeated by Pagani et al. (2015) when comparing FIR and submillimeter (sub-mm) emission across the core L183 to the 8 $\mu$m absorption map from *Spitzer* data. Fitting modified blackbody functions toward three different positions, these authors found that the contribution of a cold dust component with temperatures <10 K were not well constrained. They expressed their belief that the two cores L183 and L1689B are clear illustrations of a general problem of detecting the very cold gas mass reservoir in prestellar cores. They concluded that mass measurements based on dust emission alone might miss a large fraction of the core (30% to 70% for L183 and L1689B).

However, a detailed modeling of the filament-embedded prestellar core L1689B (Steinacker et al. 2016), based on *Herschel* PACS/SPIRE and JCMT/SCUBA-2 maps revealed that the gas mass content at temperatures <8 K is less than 10%, taking the full ambiguity of low emissivity cold dust into account. In the same work, a synergetic radiative transfer approach also allowed the investigators to derive the local ISRF of L1689B with warm and cold dust components that were a factor of 4 higher than the standard ISRF proposed by Black (1994; see also Fig. 1). This might be the main reason for Evans et al. (2001) to find the temperature in L1689B dropping below 8 K in the inner few 1000 au; these authors assumed, for their best fit, an outer field that is a factor of up to 8 lower than the field derived in Steinacker et al. (2016) based on the Herschel/JCMT maps (their Fig. 5). Differences in the assumed core and dust properties may contribute to the deviation as well. Nevertheless, even with their weak outer illumination, Evans et al. (2001) find only a gas mass of about 5% at a temperature below 8 K.

In this work, we investigate what gas mass fraction is expected to host dust at temperatures <8 K for a typical prestellar core. While we derive dust temperatures, in regions where the dust is at very low temperatures of <8 K the densities are high enough that gas and dust temperatures are the same. In this way, we estimate the very cold gas masses that contain very cold dust using the assumed gas-to-dust mass ratio (120 is used in this work). The choice of the actual value of 8 K as a border for very cold dust is somewhat arbitrary in view of the continuous decrease of the emission efficiency with temperature. We therefore follow earlier work that defined very cold dust to have temperatures up to 8 K to make the comparison easier (Pagani et al. 2015).

In Sect. 2, we define the prestellar cores, ISRF models, and dust properties, and we describe the numerical approach. Section 3 contains the obtained radial temperature profiles and mass fractions of gas with dust temperatures <8 K. We discuss the findings and present our conclusions in Sect. 4.

## 2. Models description and numerical scheme

For this assessment of typical prestellar cores, we use a simple spherically symmetric structure model although the geometry is often more complex (see, e.g., Steinacker et al. 2005). Deviations are discussed in the Sect. 4. As the $H_2$ number density profile, we choose the typical flat-to-power-law dependence of the form $n(r) = n_0/[1 + (r/r_0)^p]$ cut off at $r = R_c$ (see, e.g., Bacmann et al. 2000). The normalization $n_0$ is adjusted so that an integral over the gas in the core volume matches the chosen core mass $M_c$. The exponent $p$ is varied between 1 and 3, and the kink radius $r_0$, where the flat profile changes to the power-law profile, is chosen as $R_c/4$. Because of the observed increase of the average core radius with mass, we parameterize the outer radius as $R_c = [1+2\log_{10}(M_c/M_0)]\times10^4$ au (based on a log interpolation between cores having outer radii of $10^4$ au ($7 \times 10^4$ au) for a gas mass of 0.1 $M_\odot$ (100 $M_\odot$), respectively. The considered mass range is $M_0 = 0.1\ M_\odot$ to $M_1 = 100\ M_\odot$. The outer core radius is not well defined (Motte et al. 2007; Tan et al. 2014), but we chose the high value $7 \times 1^4$ au to consider the shielding by the outer clump as well.

Since the dust opacities are needed from the UV to the mm, we rely on the silicate and carbon data by Draine & Lee (1984) but assume an MRN size-distribution (Mathis et al. 1977) up to sizes of 0.8 $\mu$m to account for additional scattering often found in prestellar cores and interpreted to arise from coagulated grains (Steinacker et al. 2010). The resulting opacity is a about a factor of 2.5 lower than OH5 (Ossenkopf & Henning 1994) at 1 mm. The gas-to-dust mass ratio values used in the literature vary from 100 (Roy et al. 2014) over 133 (Compiègne et al. 2011) to 150 (Draine 2011). In this work we used 120. Thin ice mantles are expected to increase the opacities for the FIR/sub-mm wavelength range, however, it has to be kept in mind that the nature of the dust grains in prestellar cores is still unknown and even the various dust model opacities vary by a factor of 3.

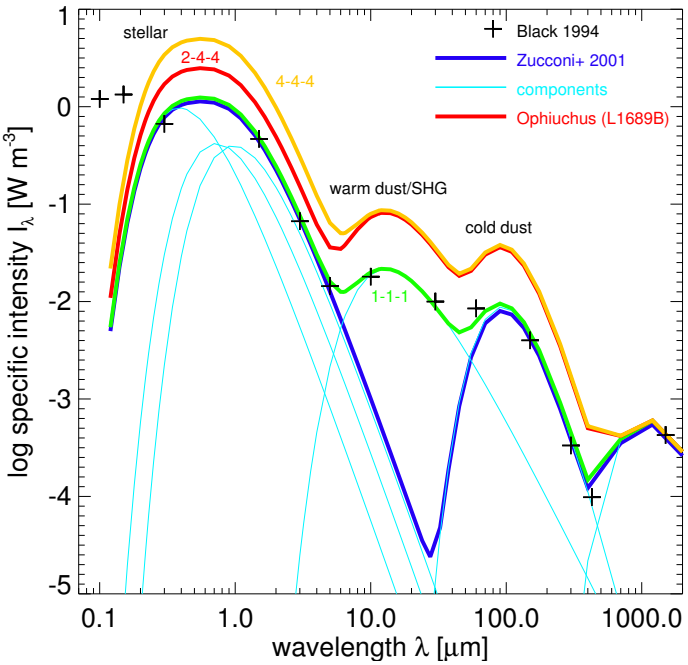


**Fig. 1.** Interstellar radiation field model featuring a stellar (I), warm dust/SHG (II), cold dust (III), and cosmic background component after Zucconi et al. (2001). The total field is shown in blue with the different components as magenta lines. A warm dust component was added to fit the data by Black (1994; plus signs). The green (orange) curve shows our low(high)-mass ISRF model, respectively (notations of the component factors: I-II-III). The red curve shows the ISRF determined for L1689B in Ophiuchus containing B stars, but not near the core (Steinacker et al. 2016).

The ISRF for low- and high-mass star formation regions is expected to show strong local variation due to nearby stellar, warm dust, or stochastically heated grain contributions, which may at shorter wavelengths be modified because of extinction and scattering. As an approximative model we used the field by Black (1994) that was modeled with single components as described in Zucconi et al. (2001). To take into account the local variations, we can multiply each of the components for stellar radiation (I), warm dust (II), and cold dust (III) by a multiplicative factor (see Fig. 1; notation for the component factors: I-II-III). Here, we discuss two cases: a typical ISRF for a low-mass star formation region (green, 1-1-1) and for a high-mass star formation region (orange, 4-4-4). As an example, we add the local field of L1689B (Steinacker et al. 2016, red, 2-4-4) indicating that PDRs strongly enhance the MIR/FIR field, but that the core is far enough from the B2 stars in that region to see just a moderate increase in the stellar component. We note that the (4-4-4) field is likely only a lower limit on the radiation field in massive star formation regions (Jørgensen et al. 2006), as these amplification factors are almost reached already, for example, in the side-complex L1689 of the Ophiuchus cloud (Steinacker et al. 2016), compared to Liseau et al. (1999) who give a single amplification factor of 10 for the main cloud part L1688. But since

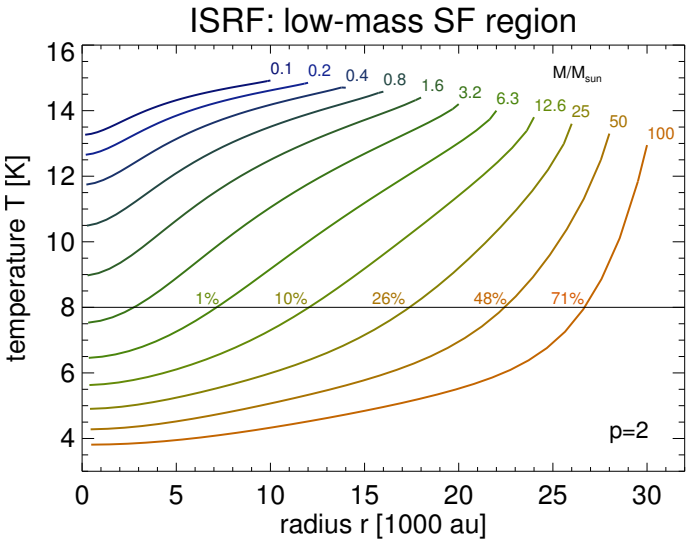


**Fig. 2.** Dust temperature profiles of cores with different total masses in a typical low-mass ISRF (1-1-1). The density power-law index was −2 ($p$ = 2) in the outer core regions. The horizontal line indicates the dust temperature limit of 8 K considered in this work; the percentage numbers indicate the fraction of mass with gas below this temperature.

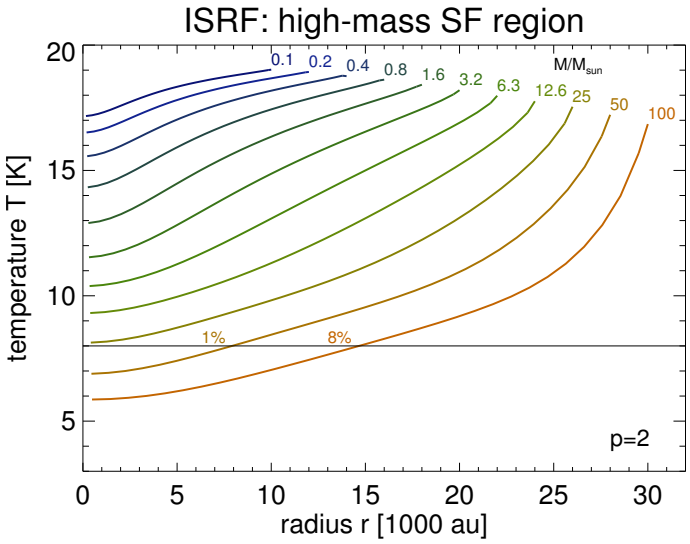


**Fig. 3.** Same as Fig. 2 for a high-mass (4-4-4)-ISRF.

we want to derive upper limits for the mass of very cold gas this is a conservative approach.

To perform a large grid of core models with different mass and outer density power-law exponent, we use a one-dimensional (1D) ray-tracing code that transports the external radiation to all core cells, and then also derives the correct dust temperature in the optically thick case by iterated cell-cell illumination. Modifications due to a three-dimensional (3D) structure are discussed in the conclusions. We include scattering in the extinction but we do not follow scattered radiation. The radiation field in the cold region (<10 K) of the cores is dominated by radiation from a wavelength range where scattering is no longer important and does not contribute to the heating. Regions where scattered radiation increases the temperature may indicate lower temperatures when scattered radiation is neglected. In the case of self-absorption (for higher mass cores) this may lead to a slight underestimation of the temperature in the outer core region that hardly affects our derived upper mass limits for very cold gas.

## 3. Radial temperature profiles and mass fractions

We first consider a low-mass star formation region characterized by a (1-1-1) ISRF. Figure 2 shows the dust temperature profiles of cores for various masses with a power-law exponent −2 (e.g., in the isothermal sphere and Bonnor-Ebert sphere model). A horizontal line at 8 K indicates at which radii the profiles enter the region of very cold dust and gas, as the gas has the same temperature as the dust. The percentage numbers give the gas mass for which the temperature is <8 K. The plot shows that cores with a total mass of 50 $M_\odot$ in a low-mass star formation region can have about half of their gas mass at $T$ < 8 K. Temperatures below 5 K are likely prevented by the action of cosmic ray heating (Evans et al. 2001, Sect. 5).

Exposed to the (4-4-4) ISRF in a high-mass star formation region, the dust temperature profiles rise compared to the low-mass case (Fig. 3). As a result, even the high-mass cores show little mass at $T$ < 8 K.

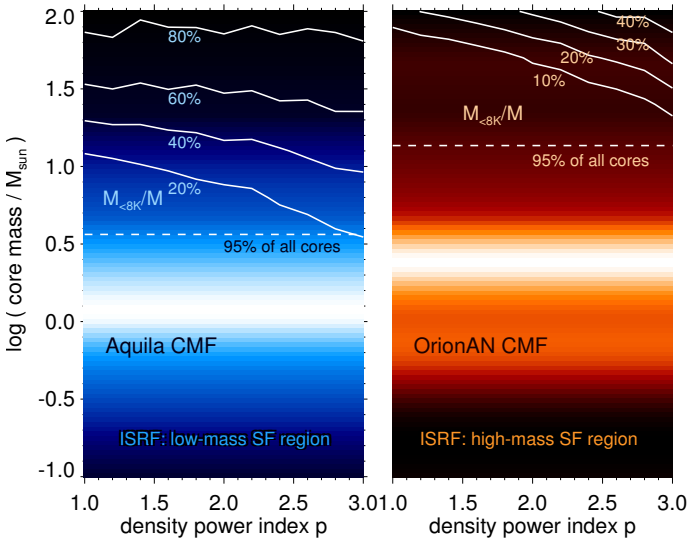


**Fig. 4.** Contours: mass fraction of gas with temperatures <8 K as a function of total core mass, and density power-index p for a low-mass star formation (1-1-1) ISRF (*left*) and a high-mass star formation (4-4-4) ISRF (*right*), respectively. Color-coded background: for each $p$, the core mass functions of Aquila (*left*) and Orion A North (*right*) are shown as a function of the core mass. Since the actual $p$ dependence is unknown, we assume that all cores have the same $p$. The dashed line indicates the mass limit below which 95% of all cores are located.

Since the temperature depends on the column density, the gradient of the density profile affects the findings. To explore this effect, we ran a grid of core masses and density power index $p$. For each core, we determined the fraction of the core gas mass with dust at temperature <8 K. The result is shown as contour lines in Fig. 4 for the low- and high-mass star formation case at left and right, respectively. The labels indicate the percentage of very cold gas. The general trend is that core with steeper density gradients show higher mass percentages of very cold gas.

To relate this limit to typical core mass distributions in the two cases, we added color-coded CMFs as background for Aquila (Orion A North) in the left (right) contour plot, respectively. Since the density power index $p$ has not been measured for all cores and likely also varies within each core, we show the color-coded CMFs along the mass axis assuming that all cores

have the same $p$. The real distribution is likely a more concentric pattern around the often observed $p = 2$. The plot shows that even when assuming a steep gradient of $p = 3$ for all cores in Aquila, the mass fraction of very cold gas hardly gets above 20% for 95% of all cores (dashed line). For the cores in the high-mass region, even the 10% limit is not reached at the extreme value of $p = 3$.

## 4. Discussion and conclusions

The variations in the local ISRF of the cores are expected to have a larger range than the two cases (1-1-1) and (4-4-4) discussed here. It is clear from the presented temperature profiles that any additional local source, such as a nearby star or PDR, further reduces the amount of very cold gas.

On the other hand, star-forming regions host also large amounts of matter shielding the core from the incoming local ISRF. This *core-external extinction* acts on top of the extinction inside the core. Zucconi et al. (2001) explicitly consider an optical extinction of 1−2 mag due to large-scale diffuse cloud dust suppressing the UV part of the Black (1994) ISRF composite. On smaller scales, filaments hosting the cores create additional increased extinction regions in the direction of the filament axis. Filaments are optically thin in low-mass star formation regions so that the MIR and FIR components that are responsible for the heating of the core center are not affected. The filament can be more opaque for high-mass star formation regions. Kainulainen et al. (2013) find for the "snake" infra-red dark cloud G11.11-0.12 that about $2 \times 10^4$ $M_\odot$ is located in the 30 pc long filament, so that a range of 1−8 mag of extinction seems possible before the radiation field can start heating the cores inside. The actual value depends on the local clumpiness in a certain direction. In turn the local MIR component in particular is also be enhanced in high-mass star formation regions. Lippok et al. (2016), for example, determined the temperature profiles of six prestellar cores with masses ranging from 2.6 to 14 $M_\odot$. Since they are located in very different environments their local fields are found to vary by application factors from 1 to 3. The derived temperature profiles show that none of the cores has a noteworthy mass fraction of gas at temperatures <8 K.

Nevertheless, there is the possibility that a low-mass core is surrounded by a more massive, but extended envelope. In this case, the shielding and thus the central temperature would be that of a more massive core. Correspondingly, the central region may host a substantial fraction of very cold gas (see Fig. 2 for masses >20 $M_\odot$). L183 is such a case with a complex gas structure of about 80 $M_\odot$ (Pagani et al. 2004) and this object is exposed to radiation that is expected to be only slightly higher than the standard ISRF (because of its elevation of 36° above the Galactic plane, but no proximity to PDRs or early-type stars, so likely a reduced warm dust component).

However, the actual 3D structure of the considered core strongly influences this. If there are "holes" allowing radiation to penetrate deeper, the temperatures remains higher (for a discussion of clumpy shells see, e.g., Indebetouw et al. 2005).

Another 3D structure effect concerns a possible fragmentation in the central few thousand au. Compared to our simple 1D model density this places more gas in better shielded regions and thus the mass in cold gas could be higher. It has to be kept in mind, however, that fragmentation in the central region does not enclose a large gas mass compared to the total core mass. Moreover, the clumpiness also allows the radiation field to penetrate deeper, which partially counteracts the stronger shielding. A precise prediction is only possible when making assumptions about the clumpiness, which is beyond the scope of this letter.

Concerning the assumed opacity, it could be argued that a higher opacity would increase extinction and therefore improve shielding and thus favor colder central temperatures. We performed tests to find out how much the obtained mass fractions of very cold dust vary with an increase in the dust opacity. We find no strong dependence on the opacity change by factors of a few. The core center is mainly heated by external FIR/mm radiation and then the balance equation from which $T$ is derived contains the opacity on both sides. For massive cores, an additional radiation source is the outer core region, where most of the UV-to-MIR radiation is converted to FIR radiation. Varying the opacity changes the temperature structure of this outer part, but only mildly changes its FIR radiation output.

In conclusion, for the bulk of cores in the low- and high-mass case we find that with reasonable assumptions about the incident local radiation field the mass fraction with dust at temperatures below 8 K exceeds 20% only for the high-mass tail of the distribution representing 5% of all cores. While this dust is more difficult to detect in FIR/sub-mm data, it comprises a small uncertainty in the total core mass determination compared to the uncertainty of the dust properties resulting in factors of a few. Also, the uncertainty from very cold gas is smaller than the uncertainties in the mass due to incorrect inclusion of surrounding filament gas, which can yield factors of 2 (see, e.g., Steinacker et al. 2016).

*Acknowledgements.* We thank the referee for very constructive comments that helped improve the paper.

## References

Alves, J., Lombardi, M., & Lada, C. J. 2007, A&A, 462, L17
Bacmann, A., André, P., Puget, J.-L., et al. 2000, A&A, 361, 555
Black, J. H. 1994, in The First Symposium on the Infrared Cirrus and Diffuse Interstellar Clouds, eds. R. M. Cutri, & W. B. Latter, ASP Conf. Ser., 58, 355
Compiègne, M., Verstraete, L., Jones, A., et al. 2011, A&A, 525, A103
Draine, B. T. 2011, Physics of the Interstellar and Intergalactic Medium (Princeton University Press)
Draine, B. T., & Lee, H. M. 1984, ApJ, 285, 89
Evans, II, N. J., Rawlings, J. M. C., Shirley, Y. L., & Mundy, L. G. 2001, ApJ, 557, 193
Indebetouw, R., Whitney, B. A., Johnson, K. E., & Wood, K. 2005, in Protostars and Planets V Posters, 1286, 8255
Jørgensen, J. K., Johnstone, D., van Dishoeck, E. F., & Doty, S. D. 2006, A&A, 449, 609
Kainulainen, J., Ragan, S. E., Henning, T., & Stutz, A. 2013, A&A, 557, A120
Könyves, V., André, P., Men'shchikov, A., et al. 2010, A&A, 518, L106
Launhardt, R., Stutz, A. M., Schmiedeke, A., et al. 2013, A&A, 551, A98
Lippok, N., Launhardt, R., Henning, T., et al. 2016, A&A, 592, A61
Liseau, R., White, G. J., Larsson, B., et al. 1999, A&A, 344, 342
Mathis, J. S., Rumpl, W., & Nordsieck, K. H. 1977, ApJ, 217, 425
Motte, F., Andre, P., & Neri, R. 1998, A&A, 336, 150
Motte, F., Bontemps, S., Schilke, P., et al. 2007, A&A, 476, 1243
Nielbock, M., Launhardt, R., Steinacker, J., et al. 2012, A&A, 547, A11
Nutter, D., & Ward-Thompson, D. 2007, MNRAS, 374, 1413
Ossenkopf, V., & Henning, T. 1994, A&A, 291, 943
Pagani, L., Bacmann, A., Motte, F., et al. 2004, A&A, 417, 605
Pagani, L., Lefèvre, C., Juvela, M., Pelkonen, V.-M., & Schuller, F. 2015, A&A, 574, L5
Roy, A., André, P., Palmeirim, P., et al. 2014, A&A, 562, A138
Shirley, Y. L., Nordhaus, M. K., Grcevich, J. M., et al. 2005, ApJ, 632, 982
Steinacker, J., Bacmann, A., Henning, T., Klessen, R., & Stickel, M. 2005, A&A, 434, 167
Steinacker, J., Pagani, L., Bacmann, A., & Guieu, S. 2010, A&A, 511, A9
Steinacker, J., Bacmann, A., Henning, T., & Heigl, S. 2016, A&A, 593, A6
Tan, J. C., Beltrán, M. T., Caselli, P., et al. 2014, Protostars and Planets VI, 149
Zucconi, A., Walmsley, C. M., & Galli, D. 2001, A&A, 376, 650